Cell Membrane-Inspired Silicone Interfaces that Mitigate Pro-inflammatory Macrophage Activation and Bacterial Adhesion

Xiao-Hua Qin[†, ‡, l,], Berna Senturk[†, ‡], Jules Valentin[†], Vera Malheiro[†], Giuseppino Fortunato[§], Qun Ren[†], Markus Rottmar[†], and Katharina Maniura-Weber[†,]**

† Laboratory for Biointerfaces
Empa, Swiss Federal Laboratories for Materials Science and Technology
Lerchenfeldstrasse 5, 9014 St Gallen, Switzerland

[l] Current address: Institute for Biomechanics, ETH Zürich, Leopold-Ruzicka-Weg 4, 8093 Zürich, Switzerland

§Laboratory for Biomimetic Membranes and Textiles
Empa, Swiss Federal Laboratories for Materials Science and Technology
Lerchenfeldstrasse 5, 9014 St Gallen, Switzerland

KEYWORDS: antifouling-antibacterial materials, macrophage polarization, surface modification, silicone, zwitterionic hydrogels

ABSTRACT

Biofouling on silicone implants causes serious complications such as fibrotic encapsulation, bacterial infection and implant failure. Here we report the development of antifouling-antibacterial silicones through covalent grafting with a cell membrane-inspired zwitterionic gel layer composed of 2-methacryolyl phosphorylcholine (MPC). To investigate how substrate properties influence cell adhesion, we cultured human blood-derived macrophages and *Escherichia coli* on polydimethylsiloxane (PDMS) and MPC gel surfaces with a range of 0.5 kPa-50 kPa in stiffness. Cells attach to glass, tissue culture polystyrene and PDMS surfaces, but they fail to form stable adhesions on MPC gel surfaces due to their superhydrophilicity and resistance to biofouling. Cytokine secretion assays confirm that MPC gels have much lower potential to trigger pro-inflammatory macrophage activation than PDMS. Finally, modification of the PDMS surface with a long-term stable hydrogel layer was achieved by surface-initiated atom transfer radical polymerization (SI-ATRP) of MPC, and confirmed by the decrease in contact angle from 110 ° to 20 °, and >70% decrease in attachment of macrophages and bacteria. This study provides new insights into the design of antifouling and antibacterial interfaces to improve the long-term biocompatibility of medical implants.

1. INTRODUCTION

Biofouling on medical devices[1-3] causes adverse complications, such as fibrotic encapsulation[1], thrombosis[4], and biomaterial-associated infection[5]. Silicone is a widely used material in medical applications due to ease of fabrication, nontoxicity, high flexibility and transparency.[6] Despite these advantages, silicone often endures a high extent of nonspecific protein fouling after implantation owing to its superhydrophobicity. Protein adsorption facilitates the attachment and activation of immune cells (macrophages), recruitment of fibroblasts, and formation of a collagen capsule around the implant. This complication has been termed as the foreign body response (FBR)[7], which significantly potentiates bacterial infections.[8] FBR-associated infections[8-9] are often promoted by bacterial attachment on surfaces[10-11] and subsequent biofilm formation.[12] Furthermore, the increasing occurrence of antimicrobial resistance[9, 13] asks for new all-in-one strategies that minimize initial attachment of immune cells and bacteria on implant surfaces to mitigate FBR and associated infection risks.

Increasing efforts have been devoted to improving the biocompatibility of silicone. Unlike most polymers, modification of poly(dimethyl siloxane) (PDMS) is a challenging task due to its low glass transition temperature (T_g). A conventional approach to prepare hydrophilic PDMS is through surface oxidization via UV-ozone or plasma treatment. While the treated surface remains hydrophilic for a period of a few minutes to hours, PDMS networks are gradually rearranged due to the low T_g (ca. -123°C) and a hydrophobic surface is regenerated in the longer term.

Recent advances in materials science have witnessed a number of antifouling materials based on neutral and zwitterionic polymer brushes.[14-15] For instance, polyethylene glycol (PEG) derivatives have been exploited to render silicon wafers, PDMS and other materials hydrophilic via silanization.[16] Zhang et al. reported a low-fouling surface based on poly(oligo(ethylene glycol) methacrylate) (POEGMA) [17] brushes grafted on silicon wafers via surface-initiated at-

om transfer radical polymerization (SI-ATRP).[17] However, PEG systems lack long-term stability since PEGs are prone to oxidative degradation.[18]

Zwitterionic molecules have shown several promising features such as superhydrophilicity, resistance to protein adsorption, and long-term stability.[19-25] Three commonly used types of zwitterionic systems are phosphorylcholine, carboxybetaines, and sulfobetaines. For instance, carboxybetaine-modified surfaces have water contact angles of less than 10° [26] and surfaces based on poly(carboxybetaine methacrylates) have shown resistance against fibrinogen adsorption for up to 74 days.[22] Recently, Jiang and co-workers reported zwitterionic polymer brushes as well as hydrogels made of polycarboxybetaines as antifouling surfaces preventing FBR.[19] Polycarboxybetaine zwitterionic hydrogels were transplanted into mice and the formation of a FBR was abolished for a period of 3 months. This success was attributed to the antifouling properties of polycarboxybetaine, which prevents nonspecific protein adsorption as well as cellular response such as macrophage activation.

While surface chemistry is an important factor for protein fouling on implants, biophysical factors such as substrate stiffness and topography have a crucial influence on cellular responses to implants.[27] Of note, macrophage attachment and activation are tightly linked to the extent of acute and chronic inflammation, fibrosis and encapsulation of implants.[28] Activated macrophages are known to express different phenotypes in response to microenvironmental signals.[29] These phenotypes have been classified as M1-like (pro-inflammatory) or M2-like (anti-inflammatory) macrophages. M1-like macrophages are crucial players in the inflammation phase during tissue injury, whereas M2-like macrophages are linked to tissue repair. The M1-like phenotype is characterized by high expression of pro-inflammatory chemokines and cytokines (e.g. IL-8, TNF-α, IL-6) and surface markers (e.g. CD197). In contrast, M2-like macrophages are associated with high expression of mannose receptors (e.g. CD206) on their surface. It is now apparent that polarized macrophages are key players of the FBR.[30] Strate-

gies reducing attachment of inflammatory cells and promoting macrophage polarization towards the M2-like phenotype at the implant interface are needed.

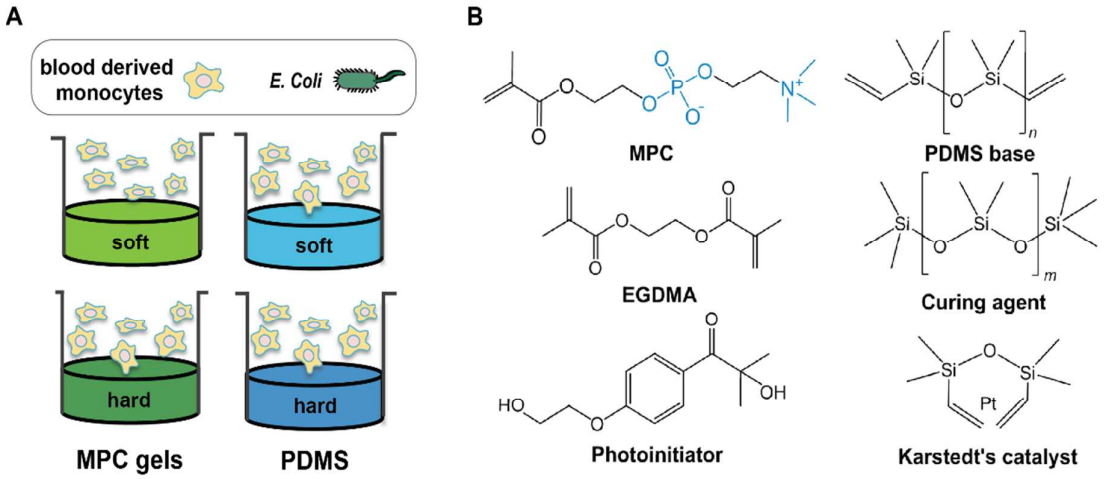

Scheme 1. A) Illustration of cell seeding on MPC gels and PDMS surfaces with varying stiffness using blood derived monocyte or *E.coli*; **B**) Chemical structures of materials used for preparing MPC and PDMS samples.

While previous studies have demonstrated the antifouling properties of cell-membrane-mimicking polymers based on 2-methacryloyloxyethyl phosphorylcholine (MPC), to date no studies have successfully transferred these functional materials onto PDMS surfaces through covalent attachment. Furthermore, a comprehensive investigation into how macrophages and bacteria interact with biomaterial surfaces are required to design long-term biocompatible implant interfaces that circumvent foreign response and bacterial infection. In this study, we report a new approach to functionalize PDMS with a stable zwitterionic hydrogel surface with antifouling and antibacterial properties. We cultured human blood-derived macrophages and Gram-negative bacteria on PDMS and zwitterionic gels composed of MPC with different degrees of stiffness (**Scheme 1**). Photocrosslinking of MPC generated cell-membrane mimicking materials that resist protein fouling. Distinct cell responses were found between PDMS and MPC gels. In contrary to PDMS, MPC gels have much lower potential to trigger pro-inflammatory macrophage activation and bacteria adhesion. Inspired by these findings, a new strategy was designed to functionalize PDMS surfaces. Firstly, an ATRP initiator was cova-

lently attached to the PDMS surface using a high M_w poly(glycidyl ether) linker. Subsequently, a zwitterionic MPC gel layer was grafted via SI-ATRP. The functionalized PDMS surface is nontoxic and shows excellent stability against protein adsorption, macrophage activation and bacterial attachment.

2. RESULTS and DISCUSSION

2.1 Materials design and characterization

To investigate how substrate properties influence cell behavior, we prepared PDMS substrates and zwitterionic MPC gels spanning a range of compliance. PDMS has been widely used for studying cell-material interactions due to its low toxicity and tunable mechanical properties. MPC is selected as the gel precursor for several reasons. MPC is a zwitterionic, cell membrane-mimicking molecule containing a hydrophilic polar head group of phospholipids and a photocrosslinkable methacrylate group. Furthermore, MPC has been previously used as coating material for improving the hemocompatibility of medical implants.[31-32] We prepared PDMS and MPC substrates with bulk stiffness (**Table 1**) in the 0.5 kPa-50 kPa range by varying the base:crosslinker (PDMS) or monomer:crosslinker (MPC) ratio from 40:1 to 10:1, respectively. The formation of MPC gels by light-initiated polymerization was monitored by real time photo-rheology as shown in **Figure 1A**. Both the kinetics of photocrosslinking and the gel moduli were determined (**Figure S1**). After UV-curing, the MPC gels were soaked in PBS solution for 4 days to reach a swelling equilibrium. It was found that the volumetric swelling ratio decreases with increasing crosslinking density (**Figure 1C**). In contrast, all PDMS samples are non-swellable in PBS due to their inherent superhydrophobicity.

Rheology measurements show that the elastic modulus (G') of PDMS and MPC gels is in the range of 0.5 – 42 kPa (**Figure 1B**), which is comparable to moduli of various soft tissues.[33] Accordingly, the theoretical mesh size of these networks is in the range of ca. 5 - 22 nm (**Table 1**).

Table 1. Properties of MPC gels and PDMS as a function of crosslinker concentration.

PDMS	base (g)	catalyst (g)	gel modulus (kPa)	mesh size (nm)	contact angle (°)
Soft	40	1	1.3 ± 0.05	14.8 ± 0.2	121.2 ± 2.6
Middle	20	1	14.1 ± 3.1	6.7 ± 0.5	118.9 ± 1.8
Hard	10	1	41.8 ± 1.4	4.6 ± 0.1	110.2 ± 2.1
MPC	**monomer (mM)**	**EGDMA (mol %)**	**gel modulus (kPa)**	**mesh size (nm)**	**contact angle (°)**
Soft	2.0	2.5	0.4 ± 0.02	21.9 ± 0.2	< 5.0
Middle	2.0	5	4.2 ± 0.1	10.0 ± 0.2	8.2 ± 1.4
Hard	2.0	10	28.7 ± 3.5	5.3 ± 0.2	18.7 ± 2.1

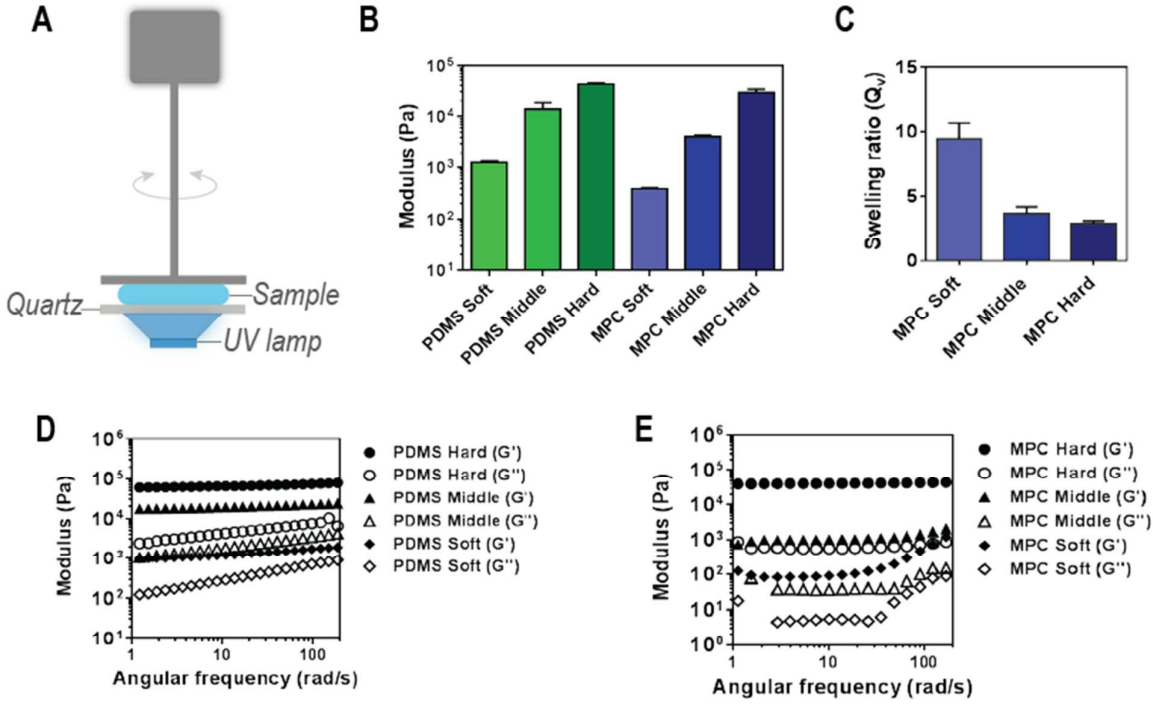

Figure 1. Physical characterization of PDMS and MPC gels. A) Schematic of plate-to-plate oscillatory rheology measurement. **B)** Elastic modulus (G') of PDMS and MPC gels measured by in situ rheology at 0.1% strain, 10 rad/s angular frequency. **C)** Volumetric swelling ratio (Q_v) of MPC gels in PBS. **D, E)** Dynamic oscillatory rheological analysis of PDMS **(D)** and MPC gels **(E)** at constant strain (0.1%) and temperature, angular frequency from 0.05 – 500 rad/s.

Next, the deformability and fluidity of PDMS and MPC gels were tested via dynamic rheometry (**Figure 1D, E**). For PDMS, G' as a measure of the stored energy by the gels during deformation were nearly independent of frequency. The viscous modulus (G'') represents the energy loss during deformation. In all measurements, G' is much higher than G'', indicating

that the elastic behavior (i.e. gel-like) is dominant over the viscous (i.e. liquid-like) behavior. For the soft PDMS, G' is frequency dependent, showing the fluidity of this material. A similar trend was observed for MPC gels with different extent of crosslinking (**Figure 1E**).

Hydrophobicity of different substrates was measured with water contact angle (**Figure S2**). PDMS substrates show contact angles in the range of 110°-120° while the MPC gels have contact angles below 20°. For PDMS, it was found that the hydrophobicity is dependent on the extent of crosslinking. For the MPC gels, the contact angle of soft gels is even not measurable due to complete wetting of the surface, indicating their superhydrophilicity.

2.2 Protein adsorption

It is generally accepted that hydrophobic surfaces absorb more proteins than hydrophilic surfaces.[34] Therefore, hydrophobic surfaces like PDMS are expected to induce much higher level of protein adsorption and cellular interactions in comparison to superhydrophilic MPC gels. To prove this hypothesis, we incubated solutions of fluorescently labelled fibrinogen with different substrates for 72 h. After thorough washing, quantification of fluorescence intensity reveals substantial levels of protein adsorption on TCP, glass and all PDMS substrates (Figure 2). In contrast, much lower extent of protein adsorption was observed on all MPC gel surfaces studied.

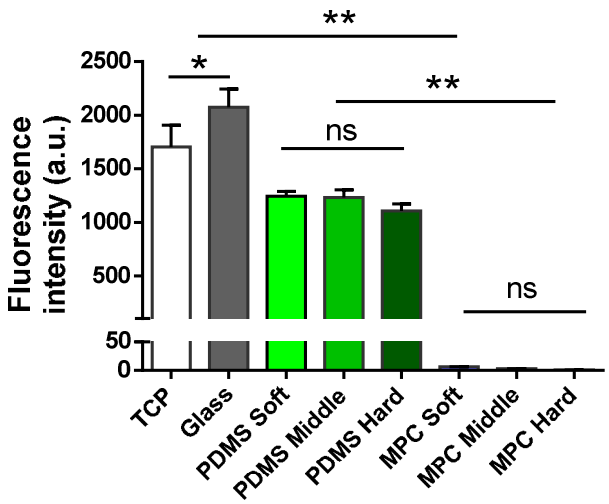

Figure 2. Protein adsorption on various susbstrates. Data presented as mean ± SD of the arbitrary units of fluorescence intensity of adsorbed Alexa-488 labelled fibrinogen. One-way ANOVA:*$P < 0.05$, **$P < 0.01$.

2.3 Macrophage-material interactions

Differentiation of monocytes into macrophages, their attachment to material surfaces and cytokine release from those cells play a key role in the inflammatory response to implanted materials and FBR. In this study, we used human blood derived monocytes, which are the first cells colonize on the surface of the implant. The use of human blood derived monocytes on FBR studies is essential since other cell types and animal studies cannot adequately recapitulate the human immune response.[35] Freshly isolated monocytes from human peripheral blood were seeded on tissue culture polystyrene (TCP), glass, PDMS and MPC substrates. Cells are firstly stimulated by macrophage colony-stimulating factor (M-CSF) for 6 days for differentiation into macrophages and then polarized for 24 h in either M1-type stimulating medium containing lipopoly-saccharides (LPS) and interferon gamma (IFN-γ) or M2-type stimulating medium containing interleukin-4 (IL-4) (**Figure 3A**).

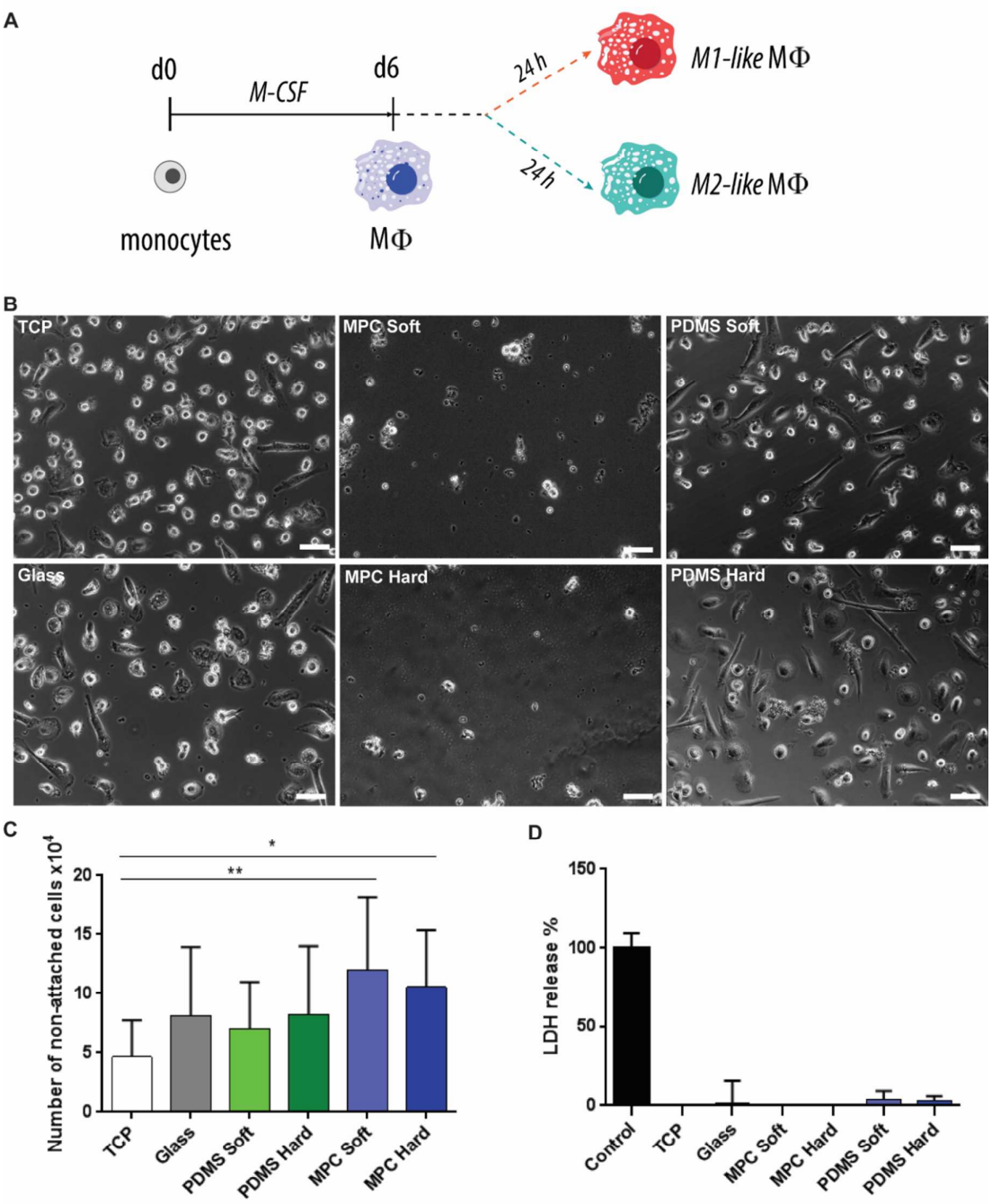

Figure 3. Macrophage-material interactions. A) Scheme of cell culture experiments. **B)** Bright-field images of macrophages after 6 d culture. **C)** Number of non-attached cells on different surfaces measured by CASY cell counter: *$P < 0.05$ and **$P < 0.01$. **D)** Cytotoxicity triggered in macrophages on different substrates measured by the LDH assay. Cells on TCP treated with lysis buffer served as positive control. Data presented as mean ± SD (n=4), scale bar= 50 µm.

Macrophage attachment and activation is crucial in the inflammatory response to implanted materials. Previous studies have shown that macrophages actively adhere to the surface of many foreign objects.[36] Macrophage attachment and morphology on various substrate types were found to be dependent on substrate stiffness and surface chemistry.[37]

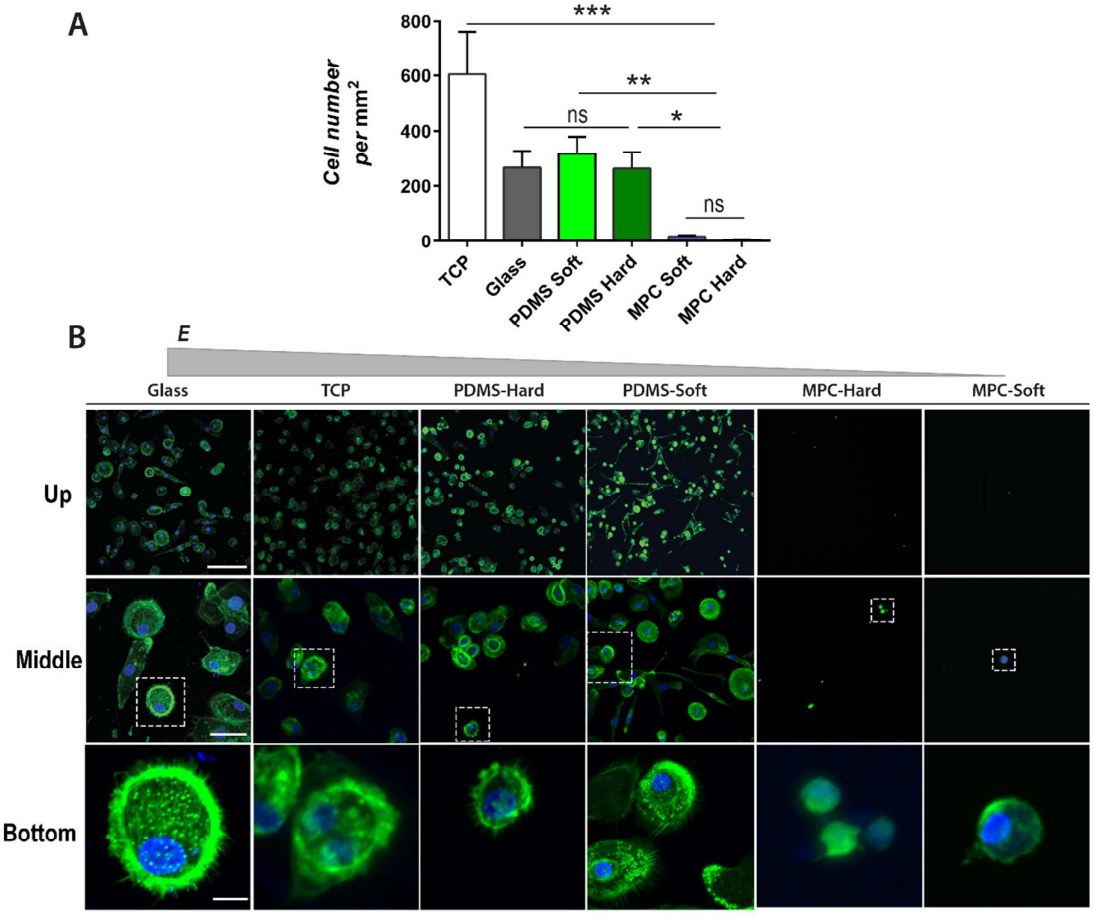

Figure 4. Quantification of cell adhesion and surface-dependent cell morphology. A) Average number of cells on different surfaces quantified by ImageJ analysis of confocal images of actin-nuclei stained macrophages on day 6, data presented as mean ± SD (n=3), $*P < 0.05$, $**P < 0.01$, $***P < 0.001$. **B)** Representative confocal images of actin/nuclei (green/blue) stained macrophages on different surfaces. Cells were imaged at low-magnification (top) and high-magnification (middle). Podosomes are shown in bottom row. Scale bars: 50 µm (top), 20 µm (middle) and 5 µm (bottom).

Figure 3B shows macrophages on different substrates in culture. While a high number of cells attached to TCP and glass (positive controls) and all types of PDMS, very few cells adhered to MPC gels. This is consistent with the quantification of non-adherent cells in the supernatants using a CASY cell counting analyzer (**Figure 3C**), showing the increased cell

number in a trend: ***TCP < soft PDMS ~ glass ~ hard PDMS < hard MPC ~ soft MPC.*** Cytotoxicity of PDMS and MPC gels was assessed via lactate dehydrogenase (LDH) assay. **Figure 3D** shows that all samples exhibit negligible toxicity to macrophages. Similar findings were also observed in a toxicity study using THP-1 cells (data not shown).

We next investigated how substrate properties influence macrophage morphology (**Figure 4**). For cells cultivated on TCP, a high number of monocytes becomes adherent after differentiation into macrophages at an average density of 655±156 cells per mm^2 (**Figure 4A**). The average cell number on different surfaces increases in a trend: ***soft MPC ~ hard MPC < soft PDMS ~ hard PDMS ~ glass < TCP.*** There was no statistical difference in cell number between glass and PDMS surfaces, but significantly fewer cells were observed on MPC gel surfaces. This is consistent with the results of non-adherent cells (**Figure 3C**) determined by CASY. High-magnification staining of the cytoskeleton shows that most macrophages have fine protrusions (podosomes) to the surfaces of glass, TCP and PDMS. However, cells seeded on MPC gels do not attach to the surface and hence do not form podosomes. While a small number of cells was observed on MPC gels during culture (**Figure 3B**), cell number was substantially reduced after washing with PBS during immunostaining, likely due to a weaker interaction with the substrate and weaker attachment. This is likely due to the superhydrophilicity of MPC gels and their robustness against protein adsorption. Cells fail to form stable adhesion on such antifouling substrates.

To study if macrophage polarization is also affected by substrate properties, at day 6 macrophage medium was changed into stimulating medium that promotes either the M1-like or M2-like phenotype. To evaluate macrophage polarization, we assessed the expression profiles of CD197 and CD206/CD163 surface markers by flow cytometry (FACS), which correspond to the pro-inflammatory (M1-like) and anti-inflammatory (M2-like) phenotype, respectively.

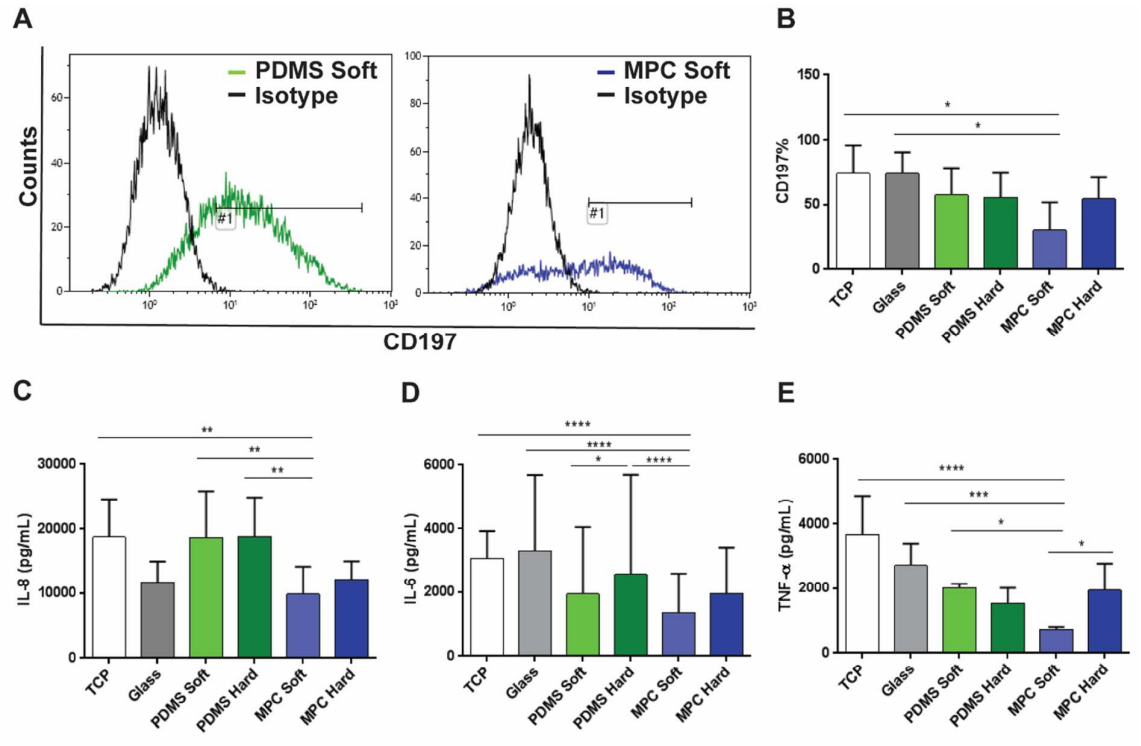

Figure 5. Macrophage polarization towards the M1-like phenotype on different surfaces. A) Representative flow cytometry histogram showing CD197 positive cells with fluorescent intensity on soft PDMS and soft MPC gel surfaces. **B)** Percentage of CD197 expression of macrophages on different surfaces after polarization, n=3, $*P < 0.05$. **C-E)** ELISA analysis of cell-secreted pro-inflammatory chemokine IL-8 (**C**), cytokines IL-6 (**D**) and TNF-α (**E**) after LPS administration. Two-way ANOVA analysis: $**P < 0.01$, $***P < 0.001$, $****P < 0.0001$.

It is appreciated that long-term presence of M1-like macrophages elicits a severe FBR, granuloma and fibrous encapsulation and eventually failure of implanted devices.[28] We measured the expression of CD197 marker on LPS- stimulated macrophages (M1-like) on different surfaces by flow cytometry (**Figure 5A-B**). It was found that macrophages on soft MPC gels had lower expression of CD197 marker compared to those on TCP, glass and PDMS.

Furthermore, we assessed the release of pro-inflammatory chemokines and cytokines IL-8, IL-6 and TNF-α by ELISA. IL-8 is a key mediator in inflammation for neutrophil recruitment and IL-8 expression is downregulated with resolution of inflammation.[38 39] **Figure 5C** shows that cells on PDMS secrete IL-8 in a similar level to those on TCP. In contrast, the level of IL-8 is significantly lower for cells on MPC gels when compared to PDMS and TCP.

IL-6 is often considered as a pro-inflammatory cytokine, can increase neutrophil production, stimulate lymphocyte proliferation and maturation, and is found at higher levels in foreign body giant cells.[40] No significant difference was found in the level of IL-6 between soft MPC and soft PDMS but cells on soft MPC expressed significantly lower amounts of IL-6 than on hard PDMS, TCP and glass surfaces (**Figure 5D**). Notably, IL-6 expression was higher on hard PDMS than soft PDMS, which correlates with the concept that pro-inflammatory mediator secretion elevates as substrate stiffness increase.[41]

Macrophage secretion of pro-inflammatory marker TNF-α (**Figure 5E**) exhibited a similar pattern to IL-6 production, with TNF-α being increased in cells on TCP and glass controls. Although no significant differences were observed for non-stimulated macrophages on different surfaces (**Figure S4**), upon LPS stimulation soft MPC gels significantly reduced the production of TNF-α when compared to soft PDMS surfaces, showing a similar trend as observed in flow cytometry analysis (**Figure 4B**). Although cells on PDMS showed higher expression of TNF-α in comparison to cells on MPC gels, their expression was significantly lower than on TCP. This is in good agreement with a report by Anderson and colleagues, who demonstrate that monocytes/macrophages seeded on PDMS express lower levels of IL-6 and TNF-α cytokines when compared to those on polystyrene control.[42] Overall, these results suggest that despite LPS and IFN-ɣ treatment, macrophages on MPC soft gels minimally polarize towards the M1 phenotype.

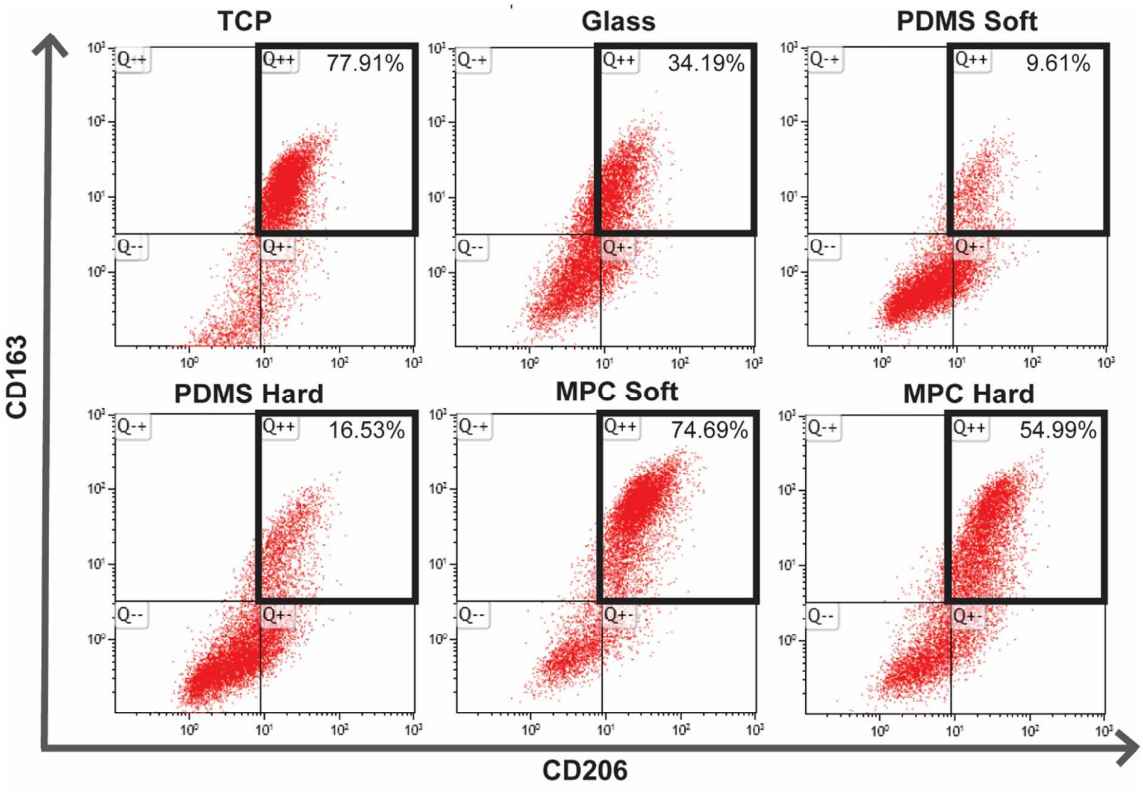

Figure 6. **Macrophage polarization towards the M2-like phenotype on different substrates.** CD163 and CD 206 surface marker expression of macrophage populations on each surface after M2 polarization.

For the Elisa analysis, it is important to note that the total levels of cytokines from different surfaces are presented without normalization to cell number (**Figure 5 C-E**). While there is an overall reduction in cytokine level on MPC gels, this result is correlated with less adherent cells (**Figure 3C**). It is probable that macrophages attached on MPC gels have very low adhesion force as they subsequently detached from the surface after medium change steps (on day 3 and day 6). Cell detachment was even more dramatic on MPC gels as seen in confocal images as a consequence of additional washing steps in immune staining **(Figure 4)**. It is already known that secretion profile differs between adherent and non-adherent macrophages.[19] Given that supernatants collected for Elisa include cytokines from both cell types, exact normalization is not feasible merely based on the number of adherent cells. However, flow cytometry

experiments are independent on cell number. The results show that in particular soft MPC gels suppress M1-like polarization (**Figure 5B**).

To further characterize macrophage populations on different surfaces, we treated cells with IL-4 to polarize them toward the M2-like phenotype. CD206, also known as MRC1 (C-type mannose receptor 1), is a 175-kDa type-I transmembrane glycoprotein that binds and internalizes glycoproteins and collagen ligands. CD163, a member of the scavenger receptor, is highly expressed in M2-like macrophages.[43] In human monocytes and tissue-resident macrophages, CD206 and CD163 expressions are amplified in response to IL-4.[44] **Figure 6** shows percentage of M2-like macrophage populations on different surfaces that are positive for both CD163 and CD206 surface markers: TCP 77.91%, Glass 34.19%, soft PDMS 9.61%, hard PDMS 16.53%, soft MPC 74.69% and hard MPC 54.99%. The soft MPC gels showed higher percentage of M2-like macrophages in comparison to PDMS. Importantly, these results correlate with reduced expression of CD197 on soft MPC gels. The phenotypical differences between soft MPC and hard MPC gels are likely due to their different stiffness. While the stiffness of TCP (ca. 1 GPa) is about one magnitude lower than that of glass (ca. 10 GPa), we observed a larger fraction of CD206 positive cells on TCP than on glass.

Differences in hydrophilicity between soft and hard MPC gels are very small, suggesting that the lower gel stiffness may account for a lower extent of cellular response on soft MPC gels. Soft MPC gels represent a promising substrate to decrease macrophage attachment, diminish the pro-inflammatory response and induce an anti-inflammatory activity with the aim to minimize FBR.

2.4 Bacteria-material interactions

Bacterial adhesion is highly dependent on substrate properties, such as hydrophobicity, charge, and topography. Here we investigated the influence of different substrates on bacterial adhesion using the Gram-negative *Escherichia coli* as a model strain.

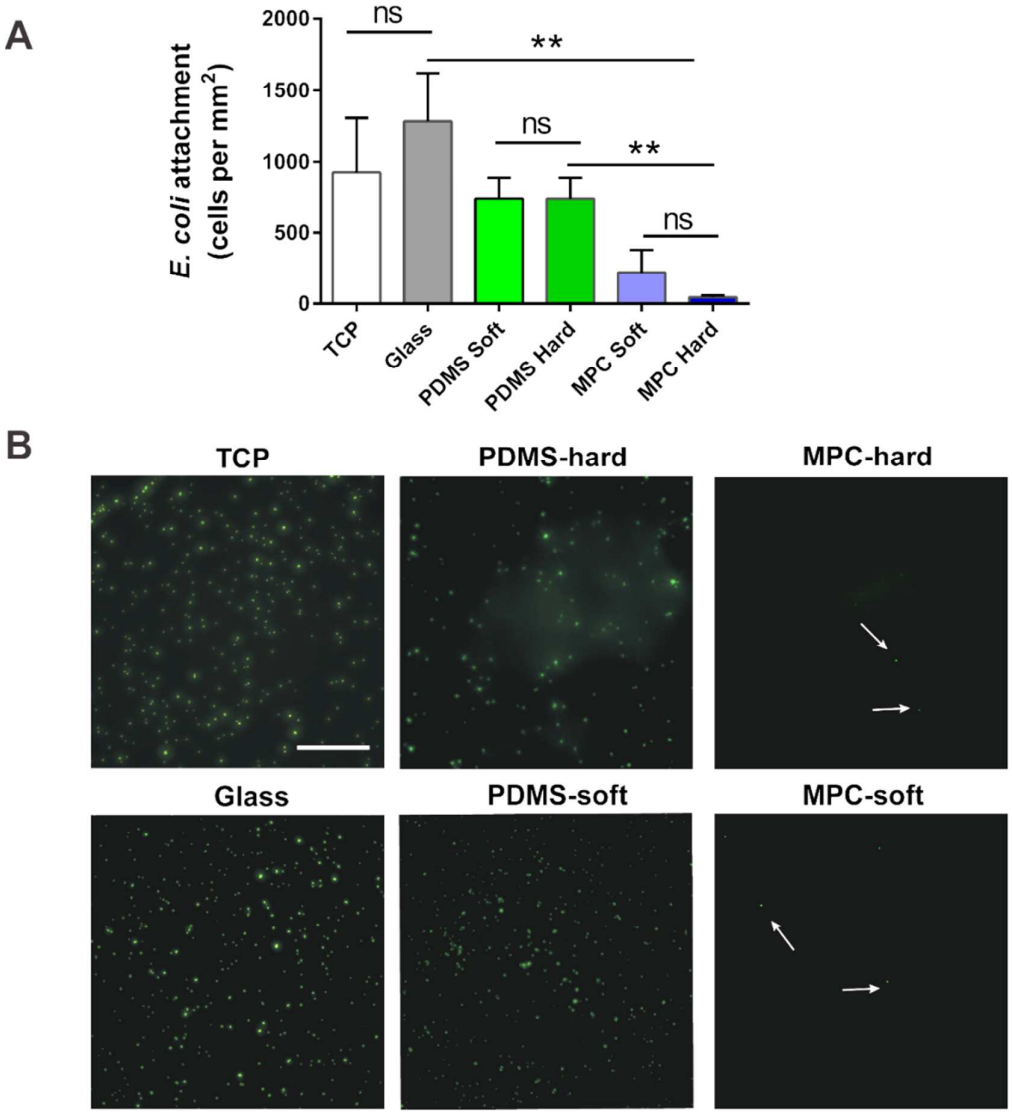

Figure 7. Bacteria adhesion on different substrates. A) The average cell number per mm^2 quantified by fluorescence imaging and ImageJ. Data presented with mean ± SD (n=3). One-way ANOVA: ns, no significant difference, $*P < 0.05$, $**P < 0.01$. **B)** Representative images of Syto9-stained E.coli on different surfaces. Arrows indicate the position of single bacteria. Scale bar, 100 µm.

After an incubation of 2 h, the adherent cells on different surfaces were stained with SYTO9. Fluorescence imaging (**Figure 7**) reveals that a high number of bacteria attached to TCP, glass and PDMS surfaces, exhibiting a high bacterial colonization with ca. 650 - 1000 cells

per mm^2. In contrast, MPC gels exhibited significantly reduced bacterial adhesion with ca. 5 - 200 cells per mm^2. These results clearly show that MPC gel surfaces strongly resist bacterial adhesion in comparison to PDMS surfaces.

2.5 Surface modification

Since MPC gels show promising features in blocking macrophage and bacteria attachment, we decided to functionalize PDMS with MPC as a superhydrophilic antifouling layer to mitigate the FBR and bacterial colonization in context with silicone substrates. Conventional methods to modify PDMS surfaces rely on plasma treatment and suffer from 'hydrophobic recovery' and lack of long term stability. In this study, we cultured macrophages on plasma-treated PDMS as the reference. A high number of adherent macrophages were observed (**Figure S3)**, indicating that conventional plasma treatment is ineffective in preparing stable hydrophilic PDMS surfaces that avoid macrophage attachment.

To address this issue, a new surface modification approach was devised in this study. Instead of immobilizing small molecules, we chose to firstly modify PDMS surfaces with a high M_w poly(glycidyl methacrylate) linker to introduce epoxide groups to stabilize the surface. It is hypothesized that this step would minimize the potential for hydrophobic recovery. Second, an ATRP initiator bearing a hydroxyl group is attached to the surface to introduce alkyl bromide groups for initiating polymerization of vinyl monomers. Finally, zwitterionic MPC hydrogels can be grafted via SI-ATRP. Importantly, SI-ATRP has been used for surface modification of glass, gold and silicon wafers with functional polymers.[14, 45]

Figure 8A depicts the procedure of a three-step surface modification approach. First, plasma-treated PDMS (PDMS-OH) was reacted with a commercial poly(glycidyl methacrylate) linker (M_n, 10-20 kDa) through a S_N2 nucleophilic substitution reaction. Second, an ATRP initiator (2-Hydroxyethyl 2-bromoisobutyrate) was immobilized on the surface under the catalysis of KOH, to generate a reactive surface (PDMS-Br).

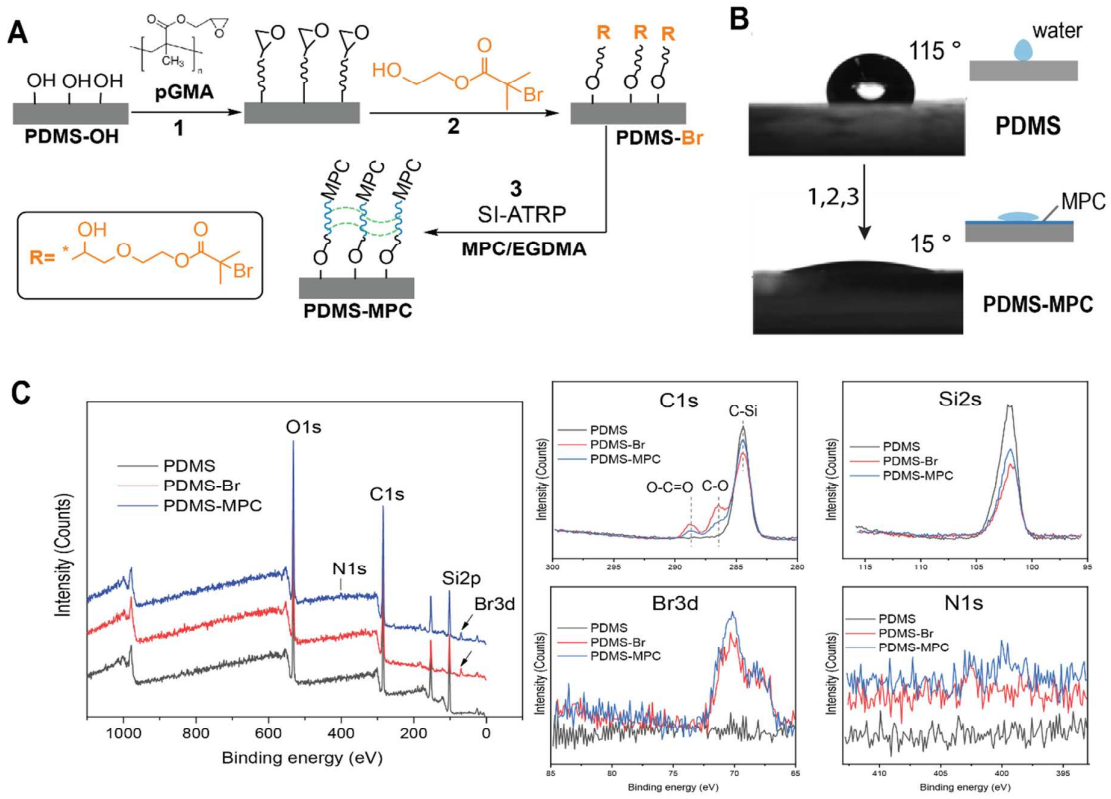

Figure 8. A) Scheme of the new surface modification strategy: **1**) plasma-treated PDMS (**PDMS-OH**) was reacted with a high M_w poly(glycidyl methacrylate) linker to introduce epoxide groups and stabilize the surface; **2**) an ATRP initiator bearing –OH groups was attached to the surface to introduce alkyl bromide groups (**PDMS-Br**); **3**) a zwitterionic hydrogel layer was grafted on PDMS-Br via SI-ATRP of MPC and EGDMA in water (**PDMS-MPC**). **B)** Water contact angle images of an unmodified PDMS surface and a MPC-grafted PDMS surface. **C)** XPS survey spectra of for PDMS, PDMS-Br and PDMS-MPC and high-resolution spectra of characteristic elemental signals: C1s, Si2s, Br3d, and N1s.

Finally, a MPC hydrogel was grafted on the surface via SI-ATRP using ethylene glycol dimethacrylate (0.1 equiv. to molar amounts of MPC) as the crosslinker. After modification, the MPC-grafted PDMS (PDMS-MPC) has a contact angle of 15° whereas the unmodified PDMS has a contact angle of ca. 115° (**Figure 8B**). After 10 weeks, the PDMS-MPC surfaces remained superhydrophilic with contact angles of ca. 18° (data not shown), indicating the success of grafting and excellent stability.

The surface chemistry of modified PDMS substrates was evaluated by XPS (**Figure 8C**) in comparison with unmodified PDMS. After immobilization of the ATRP initiator, the carbon signals at 289 (O-C=O) and 284 eV (C-O) increased significantly. These signals are associated with the organic part of the attached high M_w linker. In parallel, the intensity of C-Si and Si 2s signals decreased. Importantly, the bromine signals at 70 eV were observed on the spectrum of PDMS-Br at a concentration of 0.9 % (**Table 2**). After the grafting with MPC, we only observed a slight increase of signals corresponding to the nitrogen atoms of MPC. This might be due to the fact that an estimated detection limit for N1s signals in the range below 0.5 at.% has to be considered. However, there is a remarkable level of bromide signals on the PDMS-MPC surface, which corresponds to the residual initiating alkyl bromide group. AFM analysis (**Figure S5**) reveals that the MPC layer has an average thickness of 2-3 nm. The relatively low grafting density of MPC is likely due to the low amount of initiator immobilized on the surface, which is essential for the efficiency of SI-ATRP. Furthermore, the SI-ATRP was performed in water in which a complete removal of O_2 is more challenging compared with organic solvents.[46-47] Additional work to increase the grafting efficiency of MPC is warranted.

Table 2. Atomic concentrations on different surfaces measured by XPS.

Surfaces	C 1s (%)	O 1s (%)	Si 2p (%)	Br 3d (%)
PDMS	46.28	30.19	23.53	*ND
PDMS-Br	56.43	31.25	11.47	0.86
PDMS-MPC	55.84	29.78	13.64	0.74

**ND, not detectable*

2.6 Cell behavior on MPC-grafted PDMS

To assess if the modified PDMS-MPC surfaces have toxic effects due to the presence of initiating bromide groups, the modified samples were extracted in sterile PBS for 2 weeks. Possible cytotoxicity of the extracts was subsequently analyzed by LDH and MTS assays with human fibroblasts. Both experiments (**Figure 9A-B**) confirm that the extracts of modified PDMS are nontoxic. After seeding monocytes onto the PDMS-MPC surfaces, it was found that the MPC-grafted surfaces show the effectiveness against macrophage attachment. Confocal images of immunostained macrophages show that there is only negligible macrophage attachment on PDMS-MPC in comparison to unmodified PDMS (**Figure 9C**), being comparable to the observations on MPC gels (**Figure 4**). Importantly, ELISA analysis (**Figure 9D**) evidenced that the secretion of TNF-α is greatly suppressed on the modified surface in comparison to unmodified PDMS.

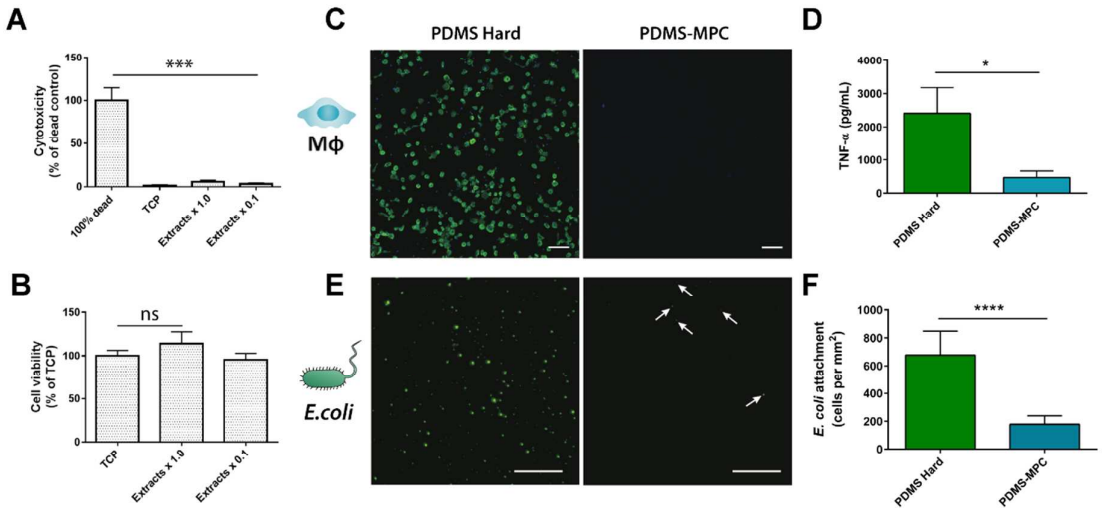

Figure 9. Biological characterization of MPC-modified PDMS. A-B) Cytotoxicity studies of extracts of MPC-modified PDMS (PDMS-MPC) surfaces measured by LDH (**A**) and MTS (**B**) assay. Data presented as mean ± SD (n=4). **C)** Confocal images of Phalloidin-stained macrophages on unmodified PDMS and MPC-modified PDMS. **D)** Analysis of cell-secreted inflammatory marker TNF-α on hard PDMS and PDMS-MPC. **E)** Fluorescent images of Syto9-stained *E.coli*. **F)** Average cell number of E.coli observed on unmodified and modified PDMS surfaces. Scale bars, 100 µm. *$P < 0.05$, **$P < 0.01$, ***$P < 0.001$, ****$P < 0.0001$

Finally, we investigated if the modified PDMS surfaces retain the antibacterial property of MPC gels. *E.coli* were seeded on PDMS and PDMS-MPC surfaces for 2h and subsequently imaged after SYTO9 staining. As shown in **Figure 9E**, a significant decrease of bacterial colonization was found on MPC-grafted PDMS surfaces (163 ± 63 cells per mm^2) when compared with unmodified PDMS surfaces (635 ± 176 cells per mm^2). These results suggest that a MPC gel layer was successfully grafted onto PDMS surfaces, remaining superhydrophilic and resistant to bacterial colonization.

3. CONCLUSION

In summary, we studied how substrate properties influence cell-material interactions such as macrophage activation and bacterial adhesion using PDMS and zwitterionic cell membrane-inspired MPC gels with varying mechanical properties. We find that MPC gel surfaces diminish cell adhesion, especially soft MPC gels inhibit expression of pro-inflammatory markers, thereby decreasing M1-like macrophage activation and favoring M2-like macrophage polarization. Furthermore, we also demonstrate that MPC gel surfaces strongly resist attachment of *E. coli*. Since MPC gels show excellent antifouling and antibacterial properties, we developed a novel approach to functionalize PDMS substrates with a long-term stable hydrogel layer composed of MPC. These new surfaces are nontoxic to mammalian cells and strongly resist macrophage attachment and bacterial colonization. This work provides new insights into the design of antifouling and antibacterial interfaces to improve the long-term biocompatibility of medical devices.

4. EXPERIMENTAL SECTION

4.1 Materials and Reagents

All materials and reagents were purchased from Sigma-Aldrich (Buchs, Switzerland) and used as received unless otherwise noted.

4.2 PDMS Preparation

PDMS composed of Sylgard 184 (Dow Corning) elastomers were prepared with different stiffness by thoroughly mixing base with curing agents at varying ratios: 40:1 (soft), 20:1 (middle), and 10:1 (hard). The base is predominantly divinyl-terminated poly(dimethylsiloxane) while the curing agent is comprised of dimethylhydrogen-terminated poly(dimethylsiloxane). The formulations were degassed for 30 min under vacuum and subsequently poured into 30 cm petri dishes. After curing at 60 °C overnight, the samples were punched into defined size (diameter 20 mm) and dried under vacuum. The samples were extracted in isopropanol for 24 h to remove uncrosslinked molecules and dried under vacuum at 50 °C for 12 h.

4.3 Hydrogel Preparation

MPC gels were prepared by photoinduced copolymerization of 2-methacryloyloxyethyl phosphorylcholine (MPC) and ethylene di-methacrylate (EDMA) as the monomer and crosslinker, respectively. To tune their mechanical properties, the molar concentration of EDMA was varied at 2.5% (soft), 5% (middle) and 10% (hard), respectively. Briefly, 807 mg of MPC and appropriate amounts of EDMA were dissolved in 0.5% Irgacure 2959 solution. After sonication for 5 min, the solutions were pipetted into a multi-well Teflon mold with a thickness of 700 μm and subsequently covered with cover slips. After UV curing for 10 min, the gels were transferred into PBS and swollen for 72 h till reaching equilibrium.

4.4 Mechanical testing

The mechanical properties of MPC gels and PDMS were measured via plate-to-plate rheometry (Anton-Paar 301, Graz). Briefly, the cylindrical samples (thickness: 0.7 mm; diameter: 20 mm) were transferred to the bottom plate. The tool-master was then positioned to 0.5 mm above the sample surface. Time-sweep rheological measurement was performed at a constant frequency of 10 rad/s and strain of 0.1 %. Elastic modulus (G') is reported as sample's stiffness. Frequency sweep measurement was run at angular frequencies of 0.05-500 rad/s and strain of 0.1 %.

The mesh size (ε) in PDMS and MPC networks was determined by the mechanical properties from rheological analysis. The complex shear modulus (G*) was determined by equation:

$$G^* = \sqrt{(G')^2 + (G'')^2}$$

where G* is the complex shear modulus, G´ is the shear storage modulus, G´´ is the shear loss modulus.

The mesh size (ε) was calculated according to equation:

$$\varepsilon = \left(\frac{6RT}{\pi N_A G^*}\right)^{1/3}$$

where T is the absolute temperature, R is the gas constant, N_A is the Avogadro's number, G* is the complex shear modulus.

4.5 Protein adsorption

Protein adsorption was measured as described elsewhere.[48] In brief, after being equilibrated in PBS at RT overnight, samples with a defined size (diameter: 10 mm) were immersed in a freshly prepared Alexa-488-labelled fibrinogen (10 µg mL^{-1}). Adsorption was allowed to proceed at RT for 2 days under gentle shaking. After four times washing with PBS, fluorescence intensity was measured on a confocal laser microscope (Zeiss LSM780) at λ_{ex}/ λ_{em} = 490 nm / 525 nm. Average fluorescence was collected from 5 positions per image (1.05 x 1.05 mm^2) in two replicates.

4.6 Cell culture and analysis

For experiments investigating macrophage attachment and polarization, human blood derived monocytes were used. Peripheral blood samples of 10 donors were obtained under informed consent according to an ethical approval (BASEC Nr. PB_2016-00816 from the local ethics committee, St. Gallen, Switzerland).

Isolation of peripheral blood mononuclear cells (PBMC) from fresh human peripheral whole blood was performed with ficoll gradient separation and monocyte isolation kit II (Miltenyi Biotec, 130-091-153) by negative selection. The magnetically labeled cells are separated from monocytes by using a MACs column. Purified monocytes were suspended in RPMI-1640 medium supplemented with 10% FBS, 2 mM L-glutamine, 100 U/mL penicillin and 100 µg/mL streptomycin. Monocytes were seeded on each surface with a cell density of 1 x 10^5 cell per cm^2. Cells were differentiated with 20 ng/mL human M-CSF (PHC9501, Invitrogen, Switzerland) for 6 days, medium was refreshed on day 3. To induce polarization, 100 ng/mL LPS (L7770, Sigma) and 20 ng/mL IFN-γ (Miltenyi Biotec) were used for M1-like polarization, 20 ng/mL IL-4 (Miltenyi Biotec) for M2-like polarization. After 7 days, supernatants were collected for ELISA analysis and macrophages were harvested by trypLE™ (12605010, Thermo Fisher Scientific) enzyme treatment and the adherent cells were collected for flow cytometry analysis.

For flow cytometry, cells were detached, washed with precooled flow cytometry buffer (PBS containing 1% BSA) and incubated on ice for 30 min with 5 µL of Fc blocking reagent human IgG (422302, Biolegend) to prevent non-specific binding of antibodies to Fc receptors. Human antibodies CD14 FITC (ab 28061, abcam), IgG1 FITC isotype control (ab 91356, abcam), CD16 APC (ab140477, abcam), IgG1 APC isotype control (ab 37391, abcam), CD206 PE (321106, Biolegend), IgG1 PE isotype control (400113, Biolegend), CD197 Alexa Fluor 647 (353218, Biolegend), IgG2a Alexa Fluor 647 isotype control (400234, Biolegend) were incubated for 45 min. After staining, cells were washed twice with flow cytometry buffer, centrifuged for 5 min and suspended in flow cytometry buffer including 3 µL of propidium iodide.

Samples were immediately run on the Gallios-Beckman Coulter flow cytometer and data was processed using Kaluza® analysis software. FL-6 (Alexa 647), FL-5 (PE-Cy7) and FL-2 (PE) channels were used for detection of CD197, CD163 and CD206 surface markers respectively. Living single cells were gated according to their forward- and side-scatter characteristics, and dead cells were excluded using propidium iodide. The positive gate was set according to the staining with the isotype control of each antibody for each group.

Cytocompatibility of MPC gels and extracts of MPC-modified PDMS was evaluated by CytoTox96® Non-Radioactive Cytotoxicity Assay. Release of lactate dehydrogenase (LDH) from damaged cells was measured by supplying lactate in the presence of diaphorase. Cell-secreted pro-inflammatory cytokines tumor necrosis factor-alpha (TNF-α), interleukin-6 (IL-6) and chemokine interleukin-8 (IL-8) were quantified by enzyme-linked immunosorbent assays (ELISA) per the manufacturers protocol.

Cells were fixed in 4% PFA, permeabilized with 0.1% Triton in PBS and finally counter-stained with Alexa-488 Phalloidin and DAPI. The samples were directly imaged on a confocal laser scanning microscope (Zeiss LSM 780).

4.7 Evaluation of Bacteria Adhesion

Escherichia coli BW25113 were used to study the interaction between bacteria and substrates. Bacterial cells at exponentially growing phase were obtained after pre-cultures in Lennox broth (LB, Roth, Germany) and were then centrifuged (4500 rpm, 4°C, 5 min), washed three successive times and suspended in phosphate-buffered saline (PBS) to an optical density of 0.01 at 600 nm, corresponding to about 5 x 10^6 colony forming units (CFU)/mL.

PDMS and MPC substrates were sterilized by UV-230nm irradiation for 30 min in 48-well plates, subsequently immerged in the bacterial suspension for 2 h at 37°C. The samples were washed in PBS for three times to remove non-adherent bacteria. The adherent bacteria were quantified with an inverted epifluorescence microscope (Nikon Eclipse Ti2, Nikon Corporation, Japan) using a 40x objective (S Plan Fluor 40x/0.60, Nikon Corporation, Japan). Bacte-

ria were fixed with 4% paraformaldehyde and 2.5% glutaraldehyde, treated with 0.1% bovine serum albumin to block the bare substrates without bacterial cells in order to reduce the background staining of SYTO9. The adherent bacteria were stained with SYTO9 (Invitrogen, S34854, USA) for 15 minutes. Five randomly acquired images having an area of 0.198 mm^2 were taken per substrate with 2 parallel replicates for each substrate. Bacterial populations from each image were quantified using ImageJ 1.50 software through direct cell counting.

4.8 Initiator immobilization

PDMS was functionalized with zwitterionic MPC layers in a multi-step procedure. First, the PDMS surface was activated using a low frequency air plasma treatment for 60 s. After activation, the sample was rinsed with ethanol for 10 min and the same procedure was repeated twice. The air-dried sample was covered with 0.5 mL of poly(glycidyl methacrylate) solution. After drying under ambient conditions for 30 min, the sample was annealed at 110 °C under N_2 protection for 30 min. Afterwards, the sample was rinsed with 2-Butanone 3 times in 15 min. After air-drying for 20 min, the sample was covered with a solution containing 20 µL of 2-Hydroxyethyl 2-bromoisobutyrate, 0.1 mL of 1 M NaOH and 0.9 mL of dimethylformamide. This reaction was performed at 70 °C for 6 h. Afterwards, the sample was rinsed with ethanol 3 times and finally air-dried for 30 min.

4.9 ATRP

Surface-initiated ATRP was performed according to a procedure adapted from Keefe et al.[20] Briefly, $Cu(II)Br_2$ (2.8 mg, 0.0125 mmol) and Cu(I)Br (7.2 mg, 0.05 mmol) were carefully placed in a Schlenk flask and sealed with septum under N_2 protection. In a large Schlenk flask, 60 mg (2.0 mmol) of MPC monomer and a PDMS substrate with immobilized initiator were placed under N_2 protection. Both flasks were deoxygenated by repeated vacuum and backfill of nitrogen. Deoxygenated water was added to the flasks: 2 mL for the first flask and 20 mL for the second flask. For preparing the metal complex, 17 µL of HMTETA was added into the

copper solution and stirred for 30 min for complexation. To initiate polymerization, 1.0 mL of the catalyst solution was added to the flask with MPC/PDMS. The reaction was maintained at room temperature for 2 h.

4.10 Surface analysis

Contact angle evaluation was performed on a Drop Shape Analyzer (DSA-100, Krüss). Atomic force microscope (AFM) analysis was performed on a Nanosurf device. The surface composition was measured using X-ray photoelectron spectroscopy (XPS) on a PHI 5000 VersaProbe II instrument (USA) with a monochromatic AlKα X-ray source. Energy resolution was set to 0.8 eV/step at a pass-energy of 187.85 eV for survey scans and 0.125 eV/step and 29.35 eV pass-energy for high resolution region scans, respectively. Carbon 1s at 284.5 eV was used as a calibration reference to correct for charge effects. Elemental compositions were determined using instrument dependent atom sensitivity factors. The photoelectron-transitions C1s, O1s, N1s, Si2p and Br3d were selected to determine the elemental concentrations and the chemical shifts within the region scans. Data analysis was performed by use of CasaXP software (Casa Software Ltd, United Kingdom).

4.11 Statistical analysis

Statistical analysis was performed using Graph Pad Prism 4.0. Student's t-test and one-way ANOVA was used for comparing differences between two groups and multiple groups, respectively. Two-way ANOVA was applied for flow cytometry and ELISA analysis.

ASSOCIATED CONTENT

Supporting figures S1-S5 contain following: rheology and contact angle measurement of different gels, confocal images of non-treated and plasma treated PDMS, TNF-alpha ELISA analysis of surfaces and AFM image of MPC-modified PDMS.

AUTHOR INFORMATION

Corresponding Author

*E-mail: xh.qin84@gmail.com (X.Q.), katharina.maniura@empa.ch (K.M.W.)

Author Contributions

‡ X.Q and B.S contributed equally to this work.

Funding Sources

X.Q. and B.S. were supported by EU Marie-Curie postdoctoral fellowship (COFUND 267161 and COFUND 754364).

Notes

The authors declare no competing financial interest.

ACKNOWLEDGMENT

The authors would like to thank Yvonne Elbs-Glatz and Ursina Tobler for support in cell culture and ELISA experiments, Alexandre Anthis for help with ATRP, Dr. Claudia Fessele for AFM, Sebastian Ulrich and Dr. Eike Müller for scientific discussions.

REFERENCES

1. Kenneth Ward, W., A review of the foreign-body response to subcutaneously-implanted devices: the role of macrophages and cytokines in biofouling and fibrosis. *Journal of diabetes science and technology* **2008,** *2* (5), 768-77.
2. Harding, J. L.; Reynolds, M. M., Combating medical device fouling. *Trends in biotechnology* **2014,** *32* (3), 140-6.
3. Magin, C. M.; Cooper, S. P.; Brennan, A. B., Non-toxic antifouling strategies. *Materials Today* **2010,** *13* (4), 36-44.
4. Leslie, D. C.; Waterhouse, A.; Berthet, J. B.; Valentin, T. M.; Watters, A. L.; Jain, A.; Kim, P.; Hatton, B. D.; Nedder, A.; Donovan, K.; Super, E. H.; Howell, C.; Johnson, C. P.; Vu, T. L.; Bolgen, D. E.; Rifai, S.; Hansen, A. R.; Aizenberg, M.; Super, M.; Aizenberg, J.; Ingber, D. E., A bioinspired omniphobic surface coating on medical devices prevents thrombosis and biofouling. *Nat Biotechnol* **2014,** *32* (11), 1134-40.
5. Damodaran, V. B.; Murthy, N. S., Bio-inspired strategies for designing antifouling biomaterials. *Biomater Res* **2016,** *20*, 18.
6. Daniels, A. U., Silicone breast implant materials. *Swiss medical weekly* **2012,** *142*, w13614.

7. Anderson, J. M.; Rodriguez, A.; Chang, D. T., Foreign body reaction to biomaterials. *Seminars in immunology* **2008,** *20* (2), 86-100.
8. Jansen, B.; Peters, G., Foreign body associated infection. *The Journal of antimicrobial chemotherapy* **1993,** *32 Suppl A*, 69-75.
9. Magill, S. S.; Edwards, J. R.; Bamberg, W.; Beldavs, Z. G.; Dumyati, G.; Kainer, M. A.; Lynfield, R.; Maloney, M.; McAllister-Hollod, L.; Nadle, J.; Ray, S. M.; Thompson, D. L.; Wilson, L. E.; Fridkin, S. K.; Emerging Infections Program Healthcare-Associated, I.; Antimicrobial Use Prevalence Survey, T., Multistate point-prevalence survey of health care-associated infections. *The New England journal of medicine* **2014,** *370* (13), 1198-208.
10. Song, F.; Ren, D., Stiffness of Cross-Linked Poly(Dimethylsiloxane) Affects Bacterial Adhesion and Antibiotic Susceptibility of Attached Cells. *Langmuir* **2014,** *30* (34), 10354-10362.
11. Weinstein, R. A.; Darouiche, R. O., Device-Associated Infections: A Macroproblem that Starts with Microadherence. *Clinical Infectious Diseases* **2001,** *33* (9), 1567-1572.
12. Magennis, E. P.; Hook, A. L.; Williams, P.; Alexander, M. R., Making Silicone Rubber Highly Resistant to Bacterial Attachment Using Thiol-ene Grafting. *ACS applied materials & interfaces* **2016,** *8* (45), 30780-30787.
13. Rossolini, G. M.; Arena, F.; Pecile, P.; Pollini, S., Update on the antibiotic resistance crisis. *Current Opinion in Pharmacology* **2014,** *18*, 56-60.
14. Chen, W.-L.; Cordero, R.; Tran, H.; Ober, C. K., 50th Anniversary Perspective: Polymer Brushes: Novel Surfaces for Future Materials. *Macromolecules* **2017,** *50* (11), 4089-4113.
15. Krishnamoorthy, M.; Hakobyan, S.; Ramstedt, M.; Gautrot, J. E., Surface-Initiated Polymer Brushes in the Biomedical Field: Applications in Membrane Science, Biosensing, Cell Culture, Regenerative Medicine and Antibacterial Coatings. *Chemical Reviews* **2014,** *114* (21), 10976-11026.
16. Plegue, T. J.; Kovach, K. M.; Thompson, A. J.; Potkay, J. A., Stability of Polyethylene Glycol and Zwitterionic Surface Modifications in PDMS Microfluidic Flow Chambers. *Langmuir : the ACS journal of surfaces and colloids* **2018,** *34* (1), 492-502.
17. Zhang, Y.; Hu, H.; Pei, X.; Liu, Y.; Ye, Q.; Zhou, F., Polymer brushes on structural surfaces: a novel synergistic strategy for perfectly resisting algae settlement. *Biomaterials Science* **2017,** *5* (12), 2493-2500.
18. Pidhatika, B.; Rodenstein, M.; Chen, Y.; Rakhmatullina, E.; Mühlebach, A.; Acikgöz, C.; Textor, M.; Konradi, R., Comparative Stability Studies of Poly(2-methyl-2-oxazoline) and Poly(ethylene glycol) Brush Coatings. *Biointerphases* **2012,** *7* (1), 1.
19. Zhang, L.; Cao, Z.; Bai, T.; Carr, L.; Ella-Menye, J. R.; Irvin, C.; Ratner, B. D.; Jiang, S., Zwitterionic hydrogels implanted in mice resist the foreign-body reaction. *Nat Biotechnol* **2013,** *31* (6), 553-6.
20. Keefe, A. J.; Brault, N. D.; Jiang, S., Suppressing surface reconstruction of superhydrophobic PDMS using a superhydrophilic zwitterionic polymer. *Biomacromolecules* **2012,** *13* (5), 1683-7.
21. Carr, L. R.; Zhou, Y.; Krause, J. E.; Xue, H.; Jiang, S., Uniform zwitterionic polymer hydrogels with a nonfouling and functionalizable crosslinker using photopolymerization. *Biomaterials* **2011,** *32* (29), 6893-9.
22. Zhang, Z.; Chao, T.; Chen, S.; Jiang, S., Superlow fouling sulfobetaine and carboxybetaine polymers on glass slides. *Langmuir : the ACS journal of surfaces and colloids* **2006,** *22* (24), 10072-7.
23. Shao, Q.; Jiang, S., Molecular understanding and design of zwitterionic materials. *Advanced materials* **2015,** *27* (1), 15-26.
24. Venault, A.; Chang, Y., Designs of Zwitterionic Interfaces and Membranes. *Langmuir* **2018**.
25. Ren, P. F.; Yang, H. C.; Liang, H. Q.; Xu, X. L.; Wan, L. S.; Xu, Z. K., Highly Stable, Protein-Resistant Surfaces via the Layer-by-Layer Assembly of Poly(sulfobetaine methacrylate) and Tannic Acid. *Langmuir* **2015,** *31* (21), 5851-8.
26. Wu, C. J.; Huang, C. J.; Jiang, S. Y.; Sheng, Y. J.; Tsao, H. K., Superhydrophilicity and spontaneous spreading on zwitterionic surfaces: carboxybetaine and sulfobetaine. *Rsc Adv* **2016,** *6* (30), 24827-24834.
27. Song, W. a. M., Joao F., Interactions between cells or proteins and surfaces exhibiting extreme wettabilities. *Soft Matter* **2013,** *9* (11), 2985-2999.

28. Sridharan, R.; Cameron, A. R.; Kelly, D. J.; Kearney, C. J.; O'Brien, F. J., Biomaterial based modulation of macrophage polarization: a review and suggested design principles. *Materials Today* **2015,** *18* (6), 313-325.
29. Vannella, K. M.; Wynn, T. A., Mechanisms of Organ Injury and Repair by Macrophages. *Annu Rev Physiol* **2017,** *79*, 593-617.
30. McWhorter, F. Y.; Davis, C. T.; Liu, W. F., Physical and mechanical regulation of macrophage phenotype and function. *Cell Mol Life Sci* **2015,** *72* (7), 1303-16.
31. Lin, X.; Fukazawa, K.; Ishihara, K., Photoreactive Polymers Bearing a Zwitterionic Phosphorylcholine Group for Surface Modification of Biomaterials. *ACS applied materials & interfaces* **2015,** *7* (31), 17489-98.
32. Goda, T.; Furukawa, H.; Gong, J. P.; Ishihara, K., Relaxation modes in chemically cross-linked poly(2-methacryloyloxyethyl phosphorylcholine) hydrogels. *Soft Matter* **2013,** *9* (7), 2166.
33. Discher, D. E.; Janmey, P.; Wang, Y. L., Tissue cells feel and respond to the stiffness of their substrate. *Science* **2005,** *310* (5751), 1139-1143.
34. Thevenot, P.; Hu, W.; Tang, L., Surface chemistry influences implant biocompatibility. *Curr Top Med Chem* **2008,** *8* (4), 270-80.
35. van Wilgenburg, B.; Browne, C.; Vowles, J.; Cowley, S. A., Efficient, long term production of monocyte-derived macrophages from human pluripotent stem cells under partly-defined and fully-defined conditions. *PLoS One* **2013,** *8* (8), e71098.
36. Vegas, A. J.; Veiseh, O.; Doloff, J. C.; Ma, M.; Tam, H. H.; Bratlie, K.; Li, J.; Bader, A. R.; Langan, E.; Olejnik, K.; Fenton, P.; Kang, J. W.; Hollister-Locke, J.; Bochenek, M. A.; Chiu, A.; Siebert, S.; Tang, K.; Jhunjhunwala, S.; Aresta-Dasilva, S.; Dholakia, N.; Thakrar, R.; Vietti, T.; Chen, M.; Cohen, J.; Siniakowicz, K.; Qi, M.; McGarrigle, J.; Graham, A. C.; Lyle, S.; Harlan, D. M.; Greiner, D. L.; Oberholzer, J.; Weir, G. C.; Langer, R.; Anderson, D. G., Combinatorial hydrogel library enables identification of materials that mitigate the foreign body response in primates. *Nat Biotechnol* **2016,** *34* (3), 345-52.
37. Blakney, A. K.; Swartzlander, M. D.; Bryant, S. J., The effects of substrate stiffness on the in vitro activation of macrophages and in vivo host response to poly(ethylene glycol)-based hydrogels. *Journal of biomedical materials research. Part A* **2012,** *100* (6), 1375-86.
38. Jones, J. A.; Chang, D. T.; Meyerson, H.; Colton, E.; Kwon, I. K.; Matsuda, T.; Anderson, J. M., Proteomic analysis and quantification of cytokines and chemokines from biomaterial surface-adherent macrophages and foreign body giant cells. *J Biomed Mater Res A* **2007,** *83* (3), 585-96.
39. Harada, A.; Sekido, N.; Akahoshi, T.; Wada, T.; Mukaida, N.; Matsushima, K., Essential involvement of interleukin-8 (IL-8) in acute inflammation. *J Leukoc Biol* **1994,** *56* (5), 559-64.
40. Neale, S. D.; Athanasou, N. A., Cytokine receptor profile of arthroplasty macrophages, foreign body giant cells and mature osteoclasts. *Acta Orthop Scand* **1999,** *70* (5), 452-8.
41. Previtera, M. L.; Sengupta, A., Substrate Stiffness Regulates Proinflammatory Mediator Production through TLR4 Activity in Macrophages. *PLoS One* **2015,** *10* (12), e0145813.
42. Anderson, J. M.; Ziats, N. P.; Azeez, A.; Brunstedt, M. R.; Stack, S.; Bonfield, T. L., Protein adsorption and macrophage activation on polydimethylsiloxane and silicone rubber. *J Biomater Sci Polym Ed* **1995,** *7* (2), 159-69.
43. Fabriek, B. O.; Dijkstra, C. D.; van den Berg, T. K., The macrophage scavenger receptor CD163. *Immunobiology* **2005,** *210* (2-4), 153-60.
44. Rőszer, T., Understanding the Mysterious M2 Macrophage through Activation Markers and Effector Mechanisms. *Mediators Inflamm* **2015,** *2015*, 816460.
45. Kawamura, A., Design of nano- and micro-structured molecule-responsive hydrogels. *Polymer Journal* **2017,** *49* (11), 751-757.
46. Matyjaszewski, K.; Miller, P. J.; Shukla, N.; Immaraporn, B.; Gelman, A.; Luokala, B. B.; Siclovan, T. M.; Kickelbick, G.; Vallant, T.; Hoffmann, H.; Pakula, T., Polymers at Interfaces: Using Atom Transfer Radical Polymerization in the Controlled Growth of Homopolymers and Block Copolymers from Silicon Surfaces in the Absence of Untethered Sacrificial Initiator. *Macromolecules* **1999,** *32* (26), 8716-8724.
47. Zoppe, J. O.; Ataman, N. C.; Mocny, P.; Wang, J.; Moraes, J.; Klok, H.-A., Surface-Initiated Controlled Radical Polymerization: State-of-the-Art, Opportunities, and Challenges in Surface and Interface Engineering with Polymer Brushes. *Chemical Reviews* **2017,** *117* (3), 1105-1318.

48. Guex, A. G.; Weidenbacher, L.; Maniura-Weber, K.; Rossi, R. M.; Fortunato, G., Hierarchical Self-Assembly of Poly(Urethane)/Poly(Vinylidene Fluoride-co-Hexafluoropropylene) Blends into Highly Hydrophobic Electrospun Fibers with Reduced Protein Adsorption Profiles. *Macromolecular Materials and Engineering* **2017,** *302* (10), 1700081.

TABLE OF CONTENTS (TOC)